

Planar cracks in the fuse model

Stefano Zapperi^{1,2}, Hans J. Herrmann², and Stéphane Roux³

¹ INFN sezione di Roma 1, Università "La Sapienza", P.le A. Moro 2 00185 Roma, Italy.

² PMMH-ESPCI, 10 Rue Vauquelin, 75231 Paris cedex 05, France

³ Laboratoire Surface du Verre et Interfaces Unité Mixte de Recherche CNRS/Saint-Gobain, 39 Quai Lucien Lefranc, BP. 135, F-93303 Aubervilliers Cedex, France.

October 27, 2018

Abstract. We simulate the propagation of a planar crack in a quasi-two dimensional fuse model, confining the crack between two horizontal plates. We investigate the effect on the roughness of microcrack nucleation ahead of the main crack and study the structure of the damage zone. The two dimensional geometry introduces a characteristic length in the problem, limiting the crack roughness. The damage ahead of the crack does not appear to change the scaling properties of the model, which are well described by gradient percolation.

PACS. 6 2.20.Fe, 62.20.Mk, 64.60.Lx

1 Introduction

Understanding the mechanisms of crack propagation is an important issue in mechanics, with potential application to geophysics and material science. Experiments have shown that in several materials under different loading conditions, the crack front tends to roughen and can often be described by self-affine scaling [1]. In particular, the *out of plane* roughness exponent is found displays universal values for a wide variety of materials [2]. Interesting experiments have been recently performed on PMMA and the *in plane* roughness of a planar crack was observed to scale with an exponent $\zeta = 0.63 \pm 0.03$ [3].

While the experimental characterization of crack roughness is quite advanced and the numerical results very accurate, theoretical understanding and numerical models are still unsatisfactory. The simplest theoretical approach to the problem identifies the crack front with a deformable line pushed by the external stress through a random toughness landscape. The deviations of the crack front from a flat line are opposed by the elastic stress field, through the stress intensity factor [4]. In certain conditions, the problem can be directly related to models and theories of interface depinning in random media and the roughness exponent computed by numerical simulations and renormalization group calculations [5,6]. Unfortunately, the agreement within this theoretical approach and experiments are quite poor. For the out of plane roughness the theory predicts only a logarithmic roughness in mode I [7], while the experimental results give $\zeta_{\perp} = 0.5$ at small length scale and $\zeta_{\perp} = 0.8$ at larger length scales [2]. For planar cracks, simulations predict $\zeta = 0.35$ [8] and RG gives $\zeta = 1/3$ [9], both quite far from the experimental result. The inclu-

sion of more details in the model, such as elastodynamic effects, does not lead to better results [9].

A different approach to crack propagation in disordered media, considers the problem from the point of view of lattice models [10]. The elastic medium is replaced by a network of bonds obeying discretized equations until the stress reached a failure threshold. The disorder in the medium can be simulated by a distribution of thresholds or by bond dilution. Models of this kind have been widely used in the past to investigate several features of fracture of disordered media, such as the failure stress [11,12,13,14], fractal properties [10,16] and avalanches [15,16,17,18,19]. The out of plane roughness exponent has been simulated in two dimension, resulting in $\zeta_{\perp} \simeq 0.7$ [20,21], and three dimensions where $\zeta_{\perp} \simeq 0.4 - 0.5$ [22,23,24]. The last result is in good agreement with experimental results, if we identify the small length scales with the quasistatic regime used in simulations. The advantage of lattice models over interface models is that the former allow for nucleation of microcracks ahead of the main crack. While it is well known experimentally that microcracks do nucleate, their effect on the roughness exponent has never been studied.

In this paper we present numerical simulations of a planar crack using the random fuse model [11]. We employ a quasi two-dimensional geometry, considering two horizontal plates separated by a network of vertical bonds. A similar setup was used in a spring model [25], but the roughness was studied only in the high velocity regime for crack motion. The experiments of Ref. [3] were instead performed at low velocity so that a quasistatic model seems more appropriate.

We find that the two dimensional geometry introduces a characteristic length limiting the crack roughness. In

addition, crack nucleation does not appear to change in a qualitative way the behavior of the system. For length scales smaller than the characteristic length, the crack is not self affine, but possibly self-similar. We study the damage zone close to the crack and find that several of its features can be described by gradient percolation [27].

2 Model

In the random fuse model, each bond of the lattice represents a fuse, that will burn when its current overcome a threshold [11,12,13,14]. The currents flowing in the lattice are obtained solving the Kirchhoff equation with appropriate boundary conditions [28]. In this paper, we consider two horizontal tilted square lattices of resistors connected by vertical fuses (see Fig. 1). The conductivity of the horizontal resistors is chosen to be unity, while the vertical fuses have conductivity σ . A voltage drop ΔV is imposed between the first horizontal rows of the plates. To simulate the propagation of a planar crack, we allow for failures of vertical bonds only and assign to each of them a random threshold j_i^c , uniformly distributed in the interval [1 : 2]. When the current in a bond i overcomes the random threshold, the bond is removed from the lattice and the currents in the lattice are recomputed, until all the currents are below the threshold. The voltage drop is thus increased until the weakest bond reaches the threshold.

The quasistatic dynamics we are using should correspond to the small constant displacement rate at the boundary of the crack used in experiments [3]. In order to avoid spurious boundary effect, we start with a preexisting crack occupying the first half of the lattice (see Fig. 1) and employ periodic boundary conditions in the direction parallel to the crack. In addition, once an entire row of fuses has failed, we shift the lattice backwards one step in the direction perpendicular to the crack, to keep the crack always in the middle of the lattice.

Before discussing the numerical results, we present some analytical considerations which will guide the simulations.

3 Characteristic length

Here we investigate the model introduced in the preceding section in some particular configuration. We first analyze the case of a perfectly straight planar crack and study the current decay in front of it. In this condition, the system is symmetric in the direction parallel to the crack and we can thus reduce it to one dimension.

We consider an infinite ladder composed of vertical bonds of resistance $r \equiv 1/\sigma$ connected by unitary horizontal resistances. Since the ladder is infinite, we can add one additional step without changing the end to end resistance R :

$$R = 2 + 1/(1/r + 1/R) = 2 + \frac{rR}{r + R}. \quad (1)$$

Solving Eq. (1) we obtain the total resistance

$$R = \sqrt{1 + 2r} + 1. \quad (2)$$

The fraction of current j flowing through the first ladder step is such that $rj = R(1 - j)$, which implies

$$j = \frac{R}{r + R} = \frac{\sqrt{1 + 2r} + 1}{r + 1 + \sqrt{1 + 2r}} = \frac{\sqrt{1 + 2r} - 1}{r}. \quad (3)$$

The current flowing in the second ladder step is then $(1 - j)j$ and similarly in the n th step it is given by $j_n = (1 - j)^{n-1}j$, thus scaling as $j_n \propto \exp(-n/\xi)$ where

$$\xi \equiv \frac{-1}{\log(1 - j)} = \frac{-1}{\log(1 - \sigma(1 - \sqrt{1 - 2/\sigma}))}. \quad (4)$$

Thus the current in front of the crack decays exponentially with a characteristic length $\xi \simeq 1/\sqrt{2\sigma}$, for $\sigma \ll 1$. A similar result could have been anticipated from the structure of the Kirchhoff equations reading as

$$\sum_{nn} (V_{i+nn} - V_i) + \sigma(V_i' - V_i) = 0 \quad (5)$$

where the sum runs over the nearest neighbors of node i and V_i' is the voltage of the corresponding node in the opposite plate. Due to symmetry we can chose $V_i' = -V_i$ and solve the equations only for one of the plates. Eq. (5) represents a discretization of a Laplace equation with a ‘‘mass term’’

$$\nabla^2 V - \xi^{-2} V = 0, \quad (6)$$

where $\xi = 1/\sqrt{2\sigma}$.

The continuum limit can be used to understand how current is transferred after a single failure. We define $G(x - x')$ as the difference in the currents in x before and after a bond in x' has failed. The function G is analogous of the ‘‘stress Green function’’ used in interface models for cracks propagation [7,8,9]. In fact, the equation of motion in these models is written as

$$\frac{\partial h(x, t)}{\partial t} = F + \int dy G(x - y)(h(y, t) - h(x, t)) + \eta(x, h), \quad (7)$$

where h indicate the position of the crack, F is proportional to the external stress, η to the random toughness of the material and for a planar crack in three dimensions $G(x) \sim 1/|x|^2$. A renormalization group analysis shows that the roughness of the interface crucially depends on the decay of G [5,6]. If G decays slower than $|x|^{-1}$, for $x \rightarrow \infty$ the interface is not rough on large length scales.

In order to compute the function G , we solve Eq. (6) with the appropriate boundary conditions. Note that by definition $G(x)$ is proportional to the differences in the voltages in x before and after removing a fuse. Since Eq. (6) is linear, the difference of the voltages still satisfies the equation in all points except $x = 0$. This condition can also be expressed in terms of the current $J \equiv \partial V / \partial y$ [26], which should be continuous everywhere apart from $x = 0$.

Let's consider a planar crack along the x direction and identify two domains:

- 1) the domain where fuses are present ($y > 0$) labeled **A**
 - 2) the domain where all fuses are burnt out ($y < 0$) labeled **B**.
- Thus the equation to solve in domain **A** is

$$\nabla^2 V = \xi^{-2} V \quad (8)$$

and in \mathbf{B} $\nabla^2 V = 0$.

Taking the Fourier transform along x , and calling k the conjugate variable to x , we can write in domain \mathbf{A}

$$\partial_y^2 \tilde{V} = (k^2 + \xi^{-2}) \tilde{V}. \quad (9)$$

Integrating the equation, setting $V \rightarrow 0$ at infinity, we obtain

$$\tilde{V}(k, y) = \tilde{V}(k, 0) \exp(-y/\ell) \quad (10)$$

where $1/\ell = \sqrt{k^2 + \xi^{-2}}$. A similar calculation allows to obtain $\tilde{V}(k, y)$ in domain \mathbf{B} .

The currents normal to the crack in the two domains are given by

$$\tilde{J}_A(k) = -\sqrt{k^2 + \xi^{-2}} \tilde{V}(k, 0) \quad (11)$$

and

$$\tilde{J}_B(k) = -|k| \tilde{V}(k, 0), \quad (12)$$

where \tilde{V} is the same for the two domains. If one bond is removed at $x = 0$ along the interface, the continuity of the current implies $J_A + J_B \sim \delta(x)$ and in Fourier space

$$\tilde{J}_A(k) + \tilde{J}_B(k) \sim 1 \quad (13)$$

and hence

$$\tilde{V} \sim \frac{-1}{|k| + \sqrt{k^2 + \xi^{-2}}}. \quad (14)$$

The Fourier transform of the function G is simply proportional to \tilde{V} and therefore at short distances $k\xi \gg 1$, $\tilde{V} \propto 1/|k|$, or $G \propto \log(x)$, while at long distances $k\xi \ll 1$, $G \propto \exp(-r/\xi)$.

We test the asymptotic behavior predicted above by estimating G from numerical simulations. The results for a lattice of size $L = 128$ are in good agreement with the analytical predictions as shown in Fig. 3. It is interesting to remark that the roughness of the crack is limited by ξ , but even in the limit $\xi \rightarrow \infty$ we do not expect a self affine crack, since G decays slower than $1/|x|$. In the next section, we will show numerically that damage nucleation does not alter this conclusion.

4 Crack roughness: simulations

In order to analyze the effect of crack nucleation ahead of the main crack, we first simulate the model confining the ruptures on the crack surface. In this way, our model reduces to a connected interface moving in a random medium with an effective stiffness given by the solution of the Kirchhoff equations. The results are then compared with simulations of the unrestricted model, where ruptures can occur everywhere in the lattice. In both cases the crack width increases with time up to a crossover time at which it saturates. In Fig. 4 we compare the damage structure in the saturated regime for the two growth rules. The height-height correlation function $C(x) \equiv \langle (h(x) - h(0))^2 \rangle$, where the average over different realizations of the disorder, is shown in Fig. 5. From these figures it is

apparent that the structure of the crack is similar in the two cases. The only difference lies in the higher saturation width that is observed when microcracks are allowed to nucleate ahead of the main crack.

Next, we analyze the behavior of the crack as a function of σ which should set the value of the characteristic length to $\xi \simeq 1/\sqrt{2\sigma}$. In this study we restrict our attention to the general model with crack nucleation. We compute the global width $W \equiv (\langle h^2 \rangle - \langle h \rangle^2)^{1/2}$, averaging over several realization of the disorder (typically 10), as a function of time for different values of ξ . Fig. 6 shows that W increases linearly in time until saturation. The global width in the saturated regime scales as ξ^ζ , with $\zeta \simeq 0.75$, as shown in Fig. 7. Due to the limited scaling range, we could not obtain a more reliable estimate of the exponent value.

5 Mean-field approach

The long-range nature of the Green function suggests that a mean-field approach could be suitable. We outline here the spirit of such an approach, through the determination of the density of burnt fuses ahead of the crack front. First, we note that the mean profile is expected to be translational invariant along the x axis and thus the problem reduces to a one dimensional geometry. As argued earlier, the tension $V(y)$ should obey the following differential equation, in the continuum limit:

$$\frac{\partial^2 V}{\partial y^2} = 2\sigma(y)V(y) \quad (15)$$

where $\sigma(y)$ is the (x -averaged) conductivity at position y . The latter can be written as $(1 - D(y))\sigma_0$ where $D(y)$ is the ‘‘damage’’, i.e. fraction of burnt fuses. This fraction is a known function of the current density in the mean-field approach. Namely, the vertical current going through intact fuses is $j(y) = 2\sigma_0 V(y) = V(y)/\xi^2$. It is remarkable that $D(y)$ drops out of this equation: the damage reduces the current density flowing at a given position by a factor $(1 - D(y))$ as compared to the intact state, but the same current density flows through a reduced number of intact fuses, and is thus multiplied by $1/(1 - D(y))$. In conclusions the two factors cancel out.

The proportion of fuses which may support the current without burning is given by the cumulative distribution of threshold currents: $P(j) = \int_j^\infty p(j')dj'$, which implies $D(y) = 1 - P(j(y))$. The voltage profile along the y axis is thus given by

$$\xi^2 \frac{\partial^2 V}{\partial y^2} = P(V(y)/\xi^2)V(y) \quad (16)$$

This equation can be rewritten in terms of the rescaled coordinate $s = y/\xi$ and current $j = V/\xi^2$ and in our case, since $P(j) = 2 - j$ for $1 < j < 2$, we obtain

$$j''(s) = j(s)(2 - j(s)). \quad (17)$$

Notice that Eq. 17 is valid only for $1 < j < 2$, while for $j < 1$ the equation becomes $j'' = j$ and for $j > 2$ we have $j'' = 0$. At infinity, $j < 1$ thus the current is given by $j = e^{-(s-s_0)}$, for $s > s_0$, so that the boundary condition for Eq. 17 at $s = s_0$ is $j(s_0) = -j'(s_0) = 1$. With these boundary conditions, Eq. (17) can not be solved explicitly so we resort to numerical integration. From the solution of Eq. (17) we obtain the damage profile and compare it to numerical simulations (see Fig. 8). The remarkable agreement between the mean-field solution and simulations, with a damage profile which is a single function of y/ξ , implies that the fracture front should be given by gradient percolation (in fact the gradient is non-linear) [27]. From this observation we can extract the scaling of the front with the gradient g (here $g \propto 1/\xi$) as $W \propto g^{-\nu/(1+\nu)} \propto \xi^{\nu/(1+\nu)}$ where ν is the percolation correlation length critical exponent $\nu = 4/3$, or $W \propto \xi^{0.57}$, reasonably consistent with our data.

6 Conclusions

In this paper, we have studied the propagation of planar cracks in the random fuse model. This model allows to investigate the effect on the crack front roughness of the microcracks nucleating ahead of the main crack. The study was restricted to a quasi two dimensional geometry and could apply to cases in which the material is very thin in the direction perpendicular to the crack plane [29].

In two dimensions, the geometry of the lattice induces a characteristic length ξ limiting the roughness and microcrack nucleation does not appear to be relevant. In addition, for length scales smaller than ξ the Green function decays very slowly, suggesting the validity of a mean-field approach. We study the problem numerically, computing the scaling of the crack width with time and ξ , and analyze the damage ahead of the crack. The results suggest an interpretation in terms of gradient percolation [27], as it is also indicated by mean-field theory. The limited range of system sizes accessible to simulations does not allow for a definite confirmation of these results.

The present analysis does not resolve the issue of the origin of the value of the roughness exponent for planar cracks in heterogeneous media. While microcrack nucleation is irrelevant in the present context, three dimensional simulations are needed to understand whether this is true in general. In principle, one could still expect that microcrack nucleation in three dimensions would change the exponent of the interface model ($\zeta = 1/3$), but the present results do not lead to such a conclusion.

Acknowledgment

S. Z. acknowledges financial support from EC TMR Research Network under contract ERBFMRXCT960062. We thank A. Baldassarri, M. Barthelemy and J. R. Rice and A. Vespignani for useful discussions.

References

1. B. B. Mandelbrot, D. E. Passoja, and A. J. Paullay, *Nature* (London) **308**, 721 (1984).
2. For a review see E. Bouchaud, *J Phys. C* **9**, 4319 (1997)
3. J. Schmittbuhl and K. Måløy, *Phys. Rev. Lett.* **78**, 3888 (1997); A. Delaplace, J. Schmittbuhl and K. J. Måløy, *Phys. Rev. E* **60**, 1337 (1999).
4. H. Gao and J. R. Rice, *ASME J. Appl. Mech.* **56**, 828 (1989).
5. T. Nattermann, S. Stepanow, L. H. Tang, and H. Leschhorn, *J. Phys. II (France)* **2**, 1483 (1992).
6. O. Narayan and D. S. Fisher, *Phys. Rev. B* **48**, 7030 (1993).
7. S. Ramanathan, D. Ertaş, and D. S. Fisher, *Phys. Rev. Lett.* **79**, 873 (1997).
8. J. Schmittbuhl, S. Roux, J. P. Vilotte, and K. J. Måløy, *Phys. Rev. Lett.* **74**, 1787 (1995); A. Tanguy, M. Gounelle and S. Roux, *Phys. Rev. E* **58**, 1577-1590, (1998).
9. S. Ramanathan and D. Fisher, *Phys. Rev. Lett.* **79**, 877 (1997); *Phys. Rev. B* **58**, 6026 (1998).
10. H.J. Herrmann and S. Roux (eds.), *Statistical Models for the Fracture of Disordered Media* (North Holland, Amsterdam, 1990).
11. L. de Arcangelis, S. Redner and H. J. Herrmann, *J. Phys. Lett. (Paris)* **46**, L585 (1985).
12. P. Duxbury, P. D. Beale and P. L. Leath, *Phys. Rev. Lett.* **57**, 1052 (1986).
13. L. de Arcangelis and H.J. Herrmann, *Phys. Rev. B* **39**, 2678 (1989).
14. B. Kahng, G. G. Batrouni, S. Redner, L. de Arcangelis and H. J. Herrmann, *Phys. Rev. B* **37**, 7625 (1988).
15. A. Hansen and P. C. Hemmer, *Phys. Lett. A* **184**, 394 (1994).
16. F. Tzschichholz and H. J. Herrmann, *Phys. Rev. E* **51**, 1961 (1995).
17. S. Zapperi, P. Ray, H. E. Stanley and A. Vespignani, *Phys. Rev. Lett.* **78**, 1408 (1997).
18. G. Caldarelli, F. Di Tolla and A. Petri *Phys. Rev. Lett.* **77**, 2503 (1996)
19. S. Zapperi, A. Vespignani and H. E. Stanley, *Nature* **388**, 658 (1997).
20. A. Hansen, E.L. Hinrichsen and S. Roux, *Phys. Rev. Lett.* **66**, 2476 (1991).
21. G. Caldarelli, R. Cafiero and A. Gabrielli, *Phys. Rev. E* **57**, 3878 (1998).
22. V. I. Raisanen, E. T. Seppala, M. J. Alava and P. M. Duxbury, *Phys. Rev. Lett.* **80**, 329 (1998).
23. G. G. Batrouni, A. Hansen, *Phys. Rev. Lett.* **80**, 325 (1998).
24. A. Parisi, G. Caldarelli and A. Pietronero, preprint.
25. T. Fukuhara and H. Nakanishi, *J. Phys. Soc. Japan* **67**, 4064 (1998).
26. We have dropped the unitary horizontal conductivity.
27. B. Sapoval, M. Rosso and J.F. Gouyet, *J. Phys. Lett. (Paris)*, **46**, L149 (1985).
28. The equations are solved numerically using a multigrid relaxation method, with precision 10^{-7} .
29. The inclusion of bending forces, which are absent in the fuse model, could change the main features of the problem. It has recently been shown that the damage ahead of the crack is irrelevant also in this case. J. Åström, M. J. Alava and J. Timonen, unpublished.

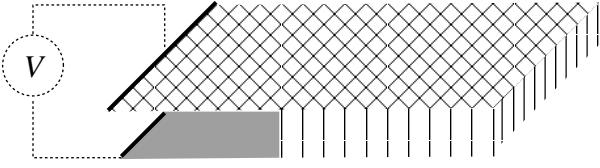


Fig. 1. The geometry of the model. The horizontal bonds have unitary conductivity while the vertical bond have conductivity σ . A planar crack is present at the center of the system and a voltage drop is applied at the boundaries.

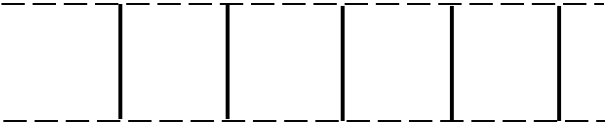


Fig. 2. The one dimensional ladder model used to compute the characteristic length. The vertical bonds have resistance r the horizontal have unitary resistance. The end to end resistance of the ladder is R .

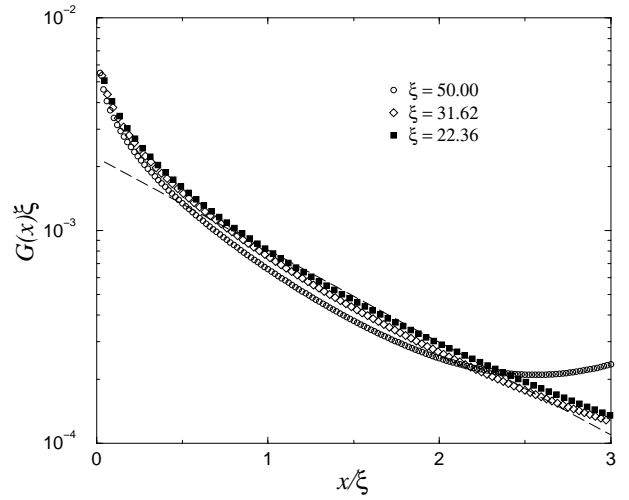
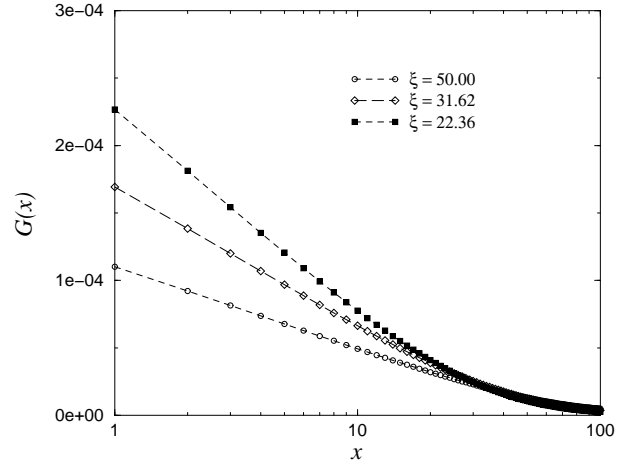


Fig. 3. The current transfer function in log-log plot (top), to show the logarithmic behavior at short length scales. In the linear-log plot (bottom) the function G has been rescaled with ξ and the collapse is in agreement with the analytical solution. The deviation from a pure exponential $\exp(-x/\xi)$, plotted as a dashed line, is due to the periodic boundary conditions employed in the simulation.

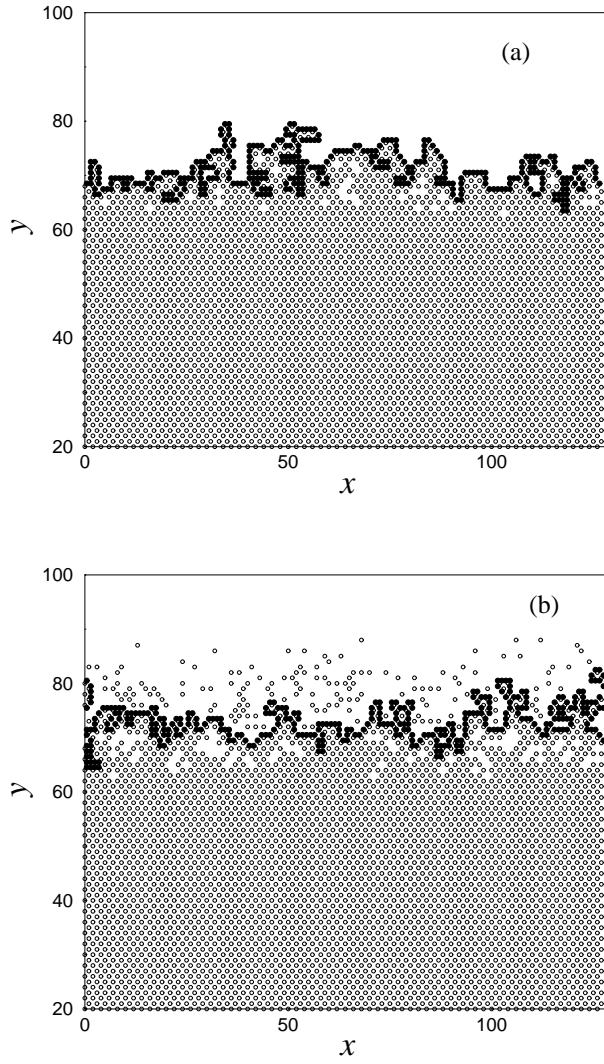


Fig. 4. The crack profiles in the steady state, when only a connected crack is allowed to grow (a) and when damage is not restricted to occur only close to the crack (b). The crack interface is shown in dark.

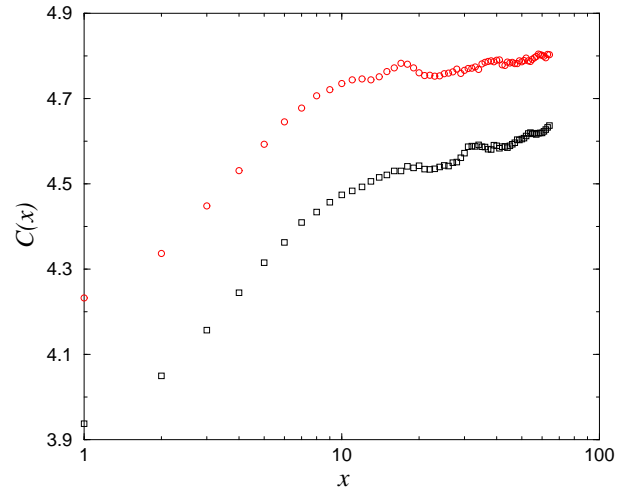


Fig. 5. Comparison between the height correlation function of a connected crack (bottom curve) and that of an unrestricted crack (upper curve).

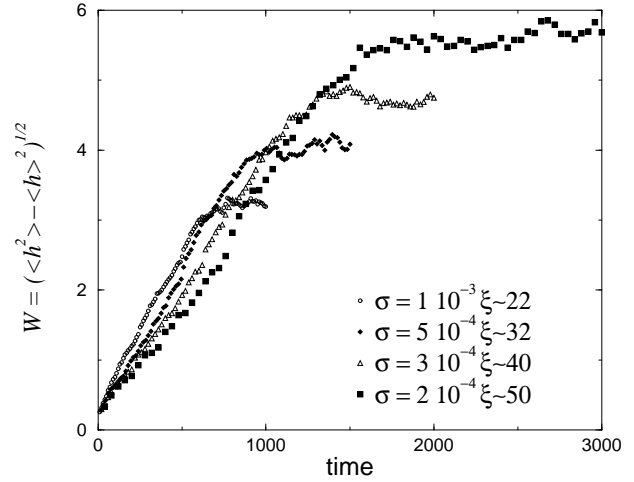


Fig. 6. The global width as a function of time for different values of σ and $\xi = 1/\sqrt{2\sigma}$.

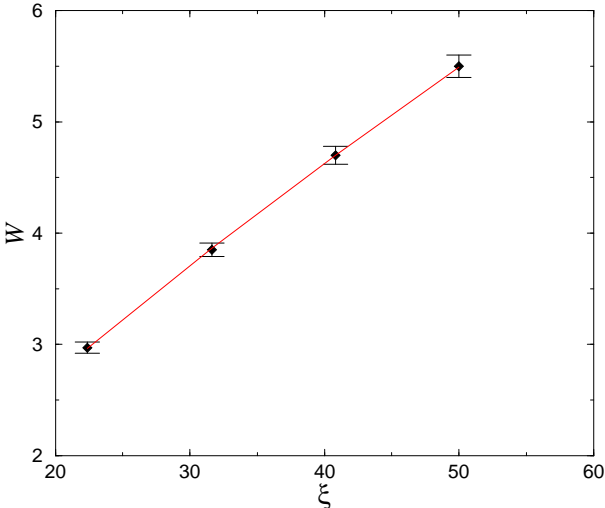


Fig. 7. The saturated global width as a function of ξ .

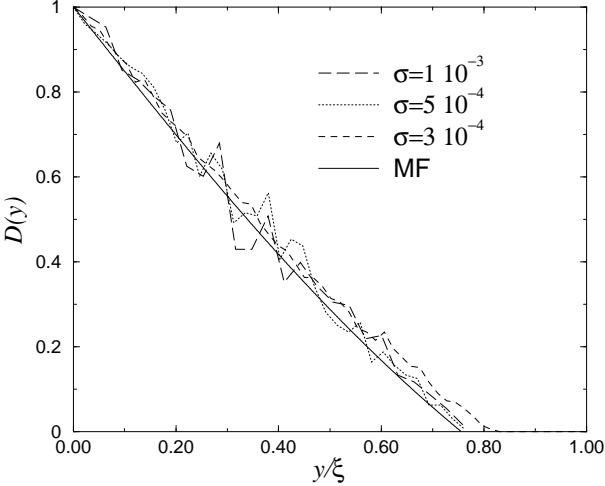


Fig. 8. The average concentration $D(y)$ of burnt fuses as a function of the reduced distance y/ξ from the crack for different values of σ . The numerical results are in excellent agreement with the mean-field solution.